JOURNAL OF BIOSCIENCE AND BIOENGINEERING
Vol. 105, No. 5, 527–535. 2008
DOI: 10.1263/jbb.105.527



# Biotin-Containing Phospholipid Vesicle Layer Formed on Self-Assembled Monolayer of a Saccharide-Terminated Alkyl Disulfide for Surface Plasmon Resonance Biosensing

Yoshiko Ishizuka-Katsura,[1] Tetsuichi Wazawa,[1§]* Tadato Ban,[2] Kenichi Morigaki,[2] and Shigeru Aoyama[1,3,4]

*OMRON-Endowed Chair in Nano Optical Devices, Graduate School of Frontier Biosciences, Osaka University, 1-3 Yamadaoka, Suita, Osaka 565-0871, Japan,[1] Research Institute for Cell Engineering, National Institute of Advanced Industrial Science and Technology, 1-8-31 Midorigaoka, Ikeda, Osaka 563-8577, Japan,[2] Advanced Device Laboratories, OMRON Corporation, 9-1 Kizugawadai, Kizu-cho, Soraku-gun, Kyoto 619-0283, Japan,[3] and CREST, JST, 4-1-8 Honcho, Kawaguchi, Saitama 332-0012, Japan[4]*

Received 29 August 2007/Accepted 19 Feburary 2008

**We describe a technique to form a biotin-containing phospholipid vesicle layer on a self-assembled monolayer (SAM) deposited on a gold surface to immobilize biotinylated receptor proteins for a surface plasmon resonance (SPR) biosensor. The adsorption of vesicle of 1,2-dioleoyl-*sn*-glycero-3-phosphocholine (DOPC) was examined by SPR on the SAMs of dithiobis(1-deoxy-glucitol-1-carbamoyl pentane) (DDGP), 11-mercaptoundecanoic acid, 11-mercaptoundecanol, 11-amino-1-undecanethiol, and 12-mercaptododecane, and it was found that the DOPC vesicle rapidly adsorbed on the DDGP SAM to achieve the highest coverage of the surface. By quartz crystal microbalance with dissipation monitoring (QCM-D), the DOPC layer formed on the DDGP SAM was shown to be a vesicle layer, in which intact DOPC vesicles physisorbed on the SAM surface. To immobilize a biotinylated receptor protein, one of three biotinylated phospholipids, 1,2-dioleoyl-*sn*-glycero-3-phosphoethanolamine-*N*-(biotinyl) (biotin-DOPE), *N*-((6-(biotinoyl)amino)hexanoyl)-1,2-dihexadecanoyl-*sn*-glycero-3-phosphoethanolamine (biotin-X-DHPE) and *N*-(biotinoyl)-1,2-dihexadecanoyl-*sn*-glycero-3-phosphoethanolamine (biotin-DHPE), was mixed with DOPC to form a biotin-containing vesicle layer on the DDGP SAM. A comparative binding study of NeutrAvidin and the biotin-containing vesicle layers showed that the use of biotin-X-DHPE achieved the most rapid immobilization of NeutrAvidin on the vesicle layer at the highest surface density. Furthermore, biotinylated protein A, as a receptor protein, could be immobilized through NeutrAvidin on the vesicle layer containing DOPC and biotin-X-DHPE, and its reaction with immunoglobulin G, as an analyte, was successfully observed by SPR. The results demonstrate that the biotin-containing vesicle layer on the DDGP SAM must be a useful component for SPR biosensor surfaces.**

[**Key words:** phospholipid, vesicle, saccharide, biotin, surface plasmon resonance, biosensor, self-assembled monolayer, protein immobilization]

Biosensor chips typically contain receptor molecules that are immobilized on a solid substrate, and the binding of analyte molecules to the receptors is measured using surface-specific analytical techniques such as surface plasmon resonance (SPR) and quartz crystal microbalance (QCM) (1). SPR is widely used for detecting biomolecular interactions on the sensor chip. SPR biosensor devices generally use the Kretschmann configuration, in which the refractive index of a layer on a noble metal film can be measured using attenuated total reflection spectroscopy (2, 3). Techniques for immobilizing receptor molecules and preventing nonspecific protein adsorption on the noble metal film have been extensively developed and investigated for biosensors (4).

Phospholipids are major components of biological membranes that compartmentalize cells and organelles. Depositing phospholipid layers on gold surfaces is of particular interest for SPR biosensors. Supported lipid membranes are one type of phospholipid self-assembly that has been extensively investigated (5–8). Typically, supported lipid membranes are prepared by applying the aqueous suspensions of phospholipid unilamellar vesicles onto solid substrates such as glasses, inducing the fusion of vesicles on the surface (9–

* Corresponding author. e-mail: wazawa@mail.tains.tohoku.ac.jp
phone/fax: +81-(0)22-795-7365
§ Present address: Laboratory of Physical Chemistry of Biomolecular Functions, Department of Materials Processing, Graduate School of Engineering, Tohoku University, 6-6-02 Aobayama, Sendai, Miyagi 980-8579, Japan; CREST, JST, 4-1-8 Honcho, Kawaguchi, Saitama 332-0012, Japan.

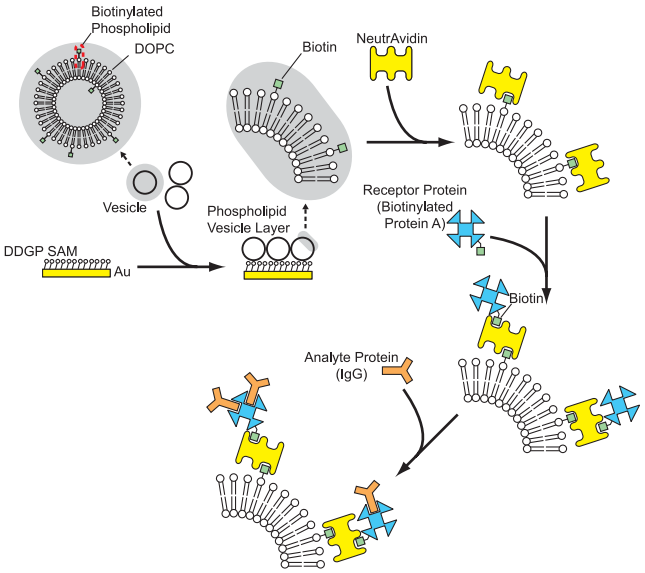


FIG. 1. Schematic diagram of SPR sensing of analyte proteins using a biotin-containing phospholipid vesicle layer.

11). The formation of planar membranes on bare gold surfaces by the vesicle fusion method has been reported to be rather difficult (12, 13), although there are some instances of successful vesicle fusion (14). Alternatively, several attempts to deposit supported lipid membranes on gold using organic self-assembled monolayers (15–20), glasslike layers (21, 22), and polymer cushions (23–25) have been reported. However, the formation of supported lipid membrane may not necessarily be essential for the surface of the SPR sensor chip, as long as the surface is resistant to nonspecific protein adsorption and capable of immobilizing specific receptor proteins without loss of their function. Some lines of research have exploited this possibility (26–30).

In this paper, we present a rather detailed study of the vesicle-based immobilization of receptor proteins for analyzing the interactions between receptor and analyte proteins by SPR (Fig. 1). To form a stable phospholipid vesicle layer on gold, we synthesized a new type of saccharide-terminated alkyl disulfide, dithiobis(1-deoxy-D-glucitol-1-carbamoyl pentane) (DDGP), and modified the gold-coated sensor surface with a hydrophilic self-assembled monolayer (SAM). SPR and QCM with dissipation monitoring (QCM-D) revealed that unilamellar vesicles of 1,2-dioleoyl-*sn*-glycero-3-phosphocholine (DOPC) adsorbed on the DDGP SAM, and the vesicle layer was stable even under the flow of a buffer solution with full coverage of the sensor chip surface. Mixed vesicles of a biotinylated phospholipid and DOPC were also found to form a vesicle layer on the DDGP SAM in a similar manner. The biotin-containing vesicle layer was able to specifically immobilize a biotinylated receptor protein through the biotin-avidin-biotin linkage and detect the interaction of analyte proteins with the receptor. We discuss several factors in the immobilization steps that are critical for the biosensing outcome.

## MATERIALS AND METHODS

**Materials** 11-Mercaptoundecanoic acid (MUA) and 11-mercaptoundecanol (MUO) were purchased from Aldrich (St. Louis, MO, USA). 11-Amino-1-undecanethiol (AUT), dithiobis(succinimidyl hexanoate) (DSH) and sulfosuccinimidyl *N*-(D-biotinyl)-6-aminohexanoate (biotin-$AC_5$-Sulfo-OSu) were purchased from Dojindo Laboratories (Kumamoto). 12-Mercaptododecane (MDD) and 1-amino-1-deoxy-D-glucitol (D-glucamine) were obtained from Tokyo Kasei Kogyo (Tokyo). Anti-bovine serum albumin antibody produced in rabbit was purchased from Sigma (St. Louis, MO, USA). Tris(hydroxymethyl)aminomethane (Tris) and protein A were purchased from Nacalai Tesque (Kyoto). DOPC, 1-palmitoyl-2-oleoyl-*sn*-glycero-3-phosphocholine (POPC) and 1,2-dioleoyl-*sn*-glycero-3-phosphoethanolamine-*N*-(biotinyl) (biotin-DOPE) were from Avanti Polar (Alabaster, AL, USA). *N*-((6-(Biotinoyl)amino) hexanoyl)-1,2-dihexadecanoyl-*sn*-glycero-3-phosphoethanolamine (biotin-X-DHPE) and *N*-(biotinoyl)-1,2-dihexadecanoyl-*sn*-glycero-3-phosphoethanolamine (biotin-DHPE) were from Invitrogen (Carlsbad, CA, USA). NeutrAvidin was from Pierce (Rockford, IL, USA). Ultrapure water was prepared using a Milli-Q Synthesis system (Millipore, Billerica, MA, USA).

**Synthesis of DDGP** A reaction to produce DDGP is shown in Fig. 2. DSH (100 mg) and D-glucamine (150 mg) were dissolved in 40 ml of *N*-dimethylformamide and 10 ml of ultrapure water, respectively. The solutions and 0.7 ml of *N*-ethyldiisoproylamine were then mixed and stirred at room temperature for 2 h, resulting in the reaction between the *N*-hydroxysuccinimidyl ester and the primary amino groups of DSH and D-glucamine, respectively. After the reaction, acetic acid (0.7 ml), ultrapure water (50 ml) and cation-exchange resin (Dowex 50WX8; Muromachi Chemicals, Fukuoka) (50 g) were added to the solution, which was gently stirred at room temperature for 30 min. The mixture was filtered and dried with a rotary evaporator. The residual solid was dissolved in 20 ml of a solvent composed of water and acetonitrile (5 : 1, v/v), and the solu-

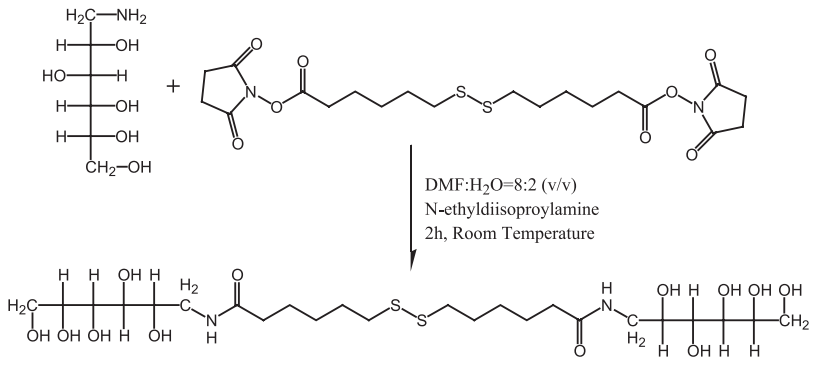


FIG. 2. Reaction scheme of the synthesis of DDGP.

tion was subjected to reverse-phase chromatography with a 626LC HPLC system (Waters, Milford, MA, USA). DDGP was isocratically eluted using a mobile phase composed of acetonitrile, water and trifluoroacetic acid (22:78:0.1, v/v) at a flow rate of 4 ml $min^{-1}$ with a Sunfire Prep C18 OBD 5-μm column (ϕ19×100 mm; Waters). The peak containing DDGP was collected and dried with a rotary evaporator. The dried DDGP was stored at −30°C. NMR spectra were measured with an Inova-600 Unityplus spectrometer (Varian, Palo Alto, CA, USA) at 25°C in DMSO-$d_6$ with tetramethylsilane as an internal standard. $^1$H-NMR (600 MHz, DMSO-$d_6$, δ): 1.29–1.34 (m, -S-$CH_2$-$CH_2$-C$H_2$-$CH_2$-$CH_2$-, 4H), 1.47–1.52 (m, -S-$CH_2$-$CH_2$-$CH_2$-C$H_2$-$CH_2$-, 4H), 1.58–1.63 (m, -S-$CH_2$-C$H_2$-$CH_2$-$CH_2$-$CH_2$-, 4H), 2.08 (t, $J$=7.5 Hz, -S-$CH_2$-$CH_2$-$CH_2$-$CH_2$-C$H_2$-, 4H), 2.69 (t, $J$=7.3 Hz, -S-C$H_2$-$CH_2$-$CH_2$-$CH_2$-$CH_2$-, 4H), 2.99–3.04 (m, H-$1_a$, 2H), 3.23–3.27 (m, H-$1_b$, 2H), 3.38 (dd, $J$=6.0, 6.1 Hz, H-$6_a$, 2H), 3.40 (dd, $J$=2.0, 1.8 Hz, H-4, 2H), 3.45–3.48 (m, H-5, 2H), 3.55–3.60 (m, H-2,3,$6_b$, 6H).

**Vesicle preparation** The desired phospholipid(s) dissolved in chloroform were transferred into an evaporation flask and dried with a rotary evaporator coupled to a vacuum pump for more than 2 h. The residual was suspended in an aqueous buffer containing 0.15 M NaCl, 10 mM Tris–HCl (pH 7.4) and 2 mM $CaCl_2$ to obtain a total phospholipid concentration of 1 mg $ml^{-1}$. Unilamellar vesicles were formed from the suspension by an extrusion method (31) with a small-volume extrusion apparatus (number of passes through a poly(carbonate) 0.05-μm filter, 19 times) (Avestin, Ontario, Canada). The vesicle suspension was stored on ice and used within 48 h.

**Deposition of self-assembled monolayers on gold-coated substrates** The surface of the gold-coated sensor chip (SIA Kit Au; Biacore, Uppsala, Sweden) was subjected to $O_2$-plasma treatment with a PICO UHP instrument (Diener Electric, Nagold, Germany) at a 30% maximal generator power for 30 s to remove organic contamination on the gold surface. A self-assembled monolayer was formed by immersing the substrate in a 1 mM solution of a thiol or disulfide derivative for more than 40 h at room temperature. The DDGP was dissolved in a mixture of acetonitrile and water (50:50, v/v) and the other derivatives were in pure ethanol. Just before use, the sensor chip was thoroughly rinsed with the solvent, ultrasonicated for 5 s with the solvent using an ultrasonication bath (W-113; Honda Electronics, Toyohashi, Aichi) at 100 kHz, rinsed with ultrapure water, and then dried under a gentle stream of class 1000 clean air.

**Biotinylation of protein A** Protein A was dissolved in a 0.1 M Hepes–NaOH buffer (pH 8.5) to yield a concentration of 10 mg $ml^{-1}$, and a 3-fold molar excess of biotin-$AC_5$-Sulfo-OSu, an amine-reactive biotinylation reagent, was added to the solution, which was gently stirred at room temperature for 3 h. The mixture was then applied to a NAP-5 column (Amersham Biosciences, Buckinghamshire, UK) equilibrated with a 20 mM Hepes–NaOH buffer (pH 7.0), and the fraction containing protein A was collected. The fraction was dialyzed against an aqueous solution containing 0.15 M NaCl, 10 mM Tris–HCl (pH 7.4) and 2 mM $CaCl_2$. The biotinylated protein A solution was frozen in liquid nitrogen and stored at −80°C. The molar ratio of bound biotin to protein A was 2.1, as measured by the HABA method (32).

**SPR measurement** SPR measurement was performed on a Biacore X instrument with a 100 μl sample loop at 25.0°C using a running buffer solution composed of 0.15 M NaCl, 10 mM Tris–HCl (pH 7.4), and 2 mM $CaCl_2$. Samples were injected at a flow rate of 5 μl $min^{-1}$. In the case of vesicles, the injection was followed by rinsing at a high flow rate of 1.5 ml $min^{-1}$ for 10 s and, subsequently, a low flow rate of 5 μl $min^{-1}$. All the samples were dialyzed against or diluted with the running buffer to minimize the change in the refractive index of the mobile phase upon injection of samples. Before injection, the injection port and the sample loop were flushed with the running buffer solution and the samples were prewarmed to room temperature.

**QCM-D measurements** QCM-D measurements were performed using a Q-Sense D300 system with a QAFC 302 axial flow chamber (Q-Sense, Västra Frölunda, Sweden). The QCM sensor crystal was oscillated at its resonance frequency of 5 MHz and at three harmonics (15, 25, and 35 MHz), and the shifts in frequency (Δf) and dissipation (ΔD) were monitored. The interval for data acquisition was 0.4 s. The clean surface of a gold-coated sensor crystal (QSX 301; Q-Sense) was treated with a solution of 1 mM DDGP in acetonitrile/water solution (50:50, v/v), similarly to the treatment of the gold-coated SPR sensor chips as described earlier (see Deposition of self-assembled monolayers on gold-coated substrates).

**Nonlinear least-square estimation** The SPR signal curves of NeutrAvidin binding were fitted with a function,

$$y_0 - A_1 \exp(-k_1(t-t_0)) - A_2 \exp(-k_2(t-t_0)) \quad (1)$$

where $y_0$ is an SPR signal when the binding of NeutrAvidin reaches a plateau, $t_0$ is the time when the injection of NeutrAvidin was started, and $A_1$ and $A_2$ are the increases in the SPR signal due to the binding of NeutrAvidin to the biotin-containing vesicle layers at rate constants of $k_1$ and $k_2$, respectively. The nonlinear least-square fitting was performed using Origin software, ver. 7J (OriginLab, Northampton, MA, USA).

## RESULTS

**Adsorption of vesicles onto SAMs** We examined the adsorption of the DOPC vesicle on the SAMs of disulfide and thiol derivatives: DDGP, MUO, MUA, AUT and MDD with glucitol, hydroxyl, carboxyl, amino and methyl terminal groups, respectively (Fig. 3A). A gold-coated SPR sensor chip was treated with a solution of one of the reagents to form a SAM on the chip surface. After the sensor chip substrate was mounted on the Biacore SPR instrument, the DOPC vesicle suspension was injected, and the SPR signal was recorded as a function of time. During injection, the SPR signal increased owing to its adsorption on the SAM (Fig. 3B). The SPR signal rapidly increased and reached a plateau when the DOPC vesicle was applied to the sensor chips of DDGP, MUO and MUA SAMs. In contrast, the SPR signal increased more slowly when the DOPC vesicle was applied to the sensor chips of MDD and AUT SAMs. Following the injection of the DOPC vesicle, the sensor chip surface was rinsed with the running buffer at a high flow rate of 1.5 ml $min^{-1}$ for 10 s and, subsequently, at a low flow rate of 5 μl $min^{-1}$. SPR signals for the SAMs of DDGP, MUO and MUA were unaffected by the rinses, but the SPR signals for the SAMs of MDD and AUT rapidly decreased during the high-flow-rate rinse and then gradually decreased during the low-flow-rate rinse. Furthermore, the SPR signal after the end of the DOPC vesicle injection for DDGP SAM is higher than those for MUO and MUA SAMs (Fig. 3B), suggesting the highest coverage of DOPC for the DDGP SAM.

The adsorption of the DOPC vesicle on the DDGP SAM was investigated by QCM-D. The DOPC vesicle suspension was applied to the DDGP SAM deposited on a gold-coated sensor crystal, and the shifts in both resonance frequency and dissipation were measured as functions of time. After the injection of the DOPC vesicle, the shifts in both reso-

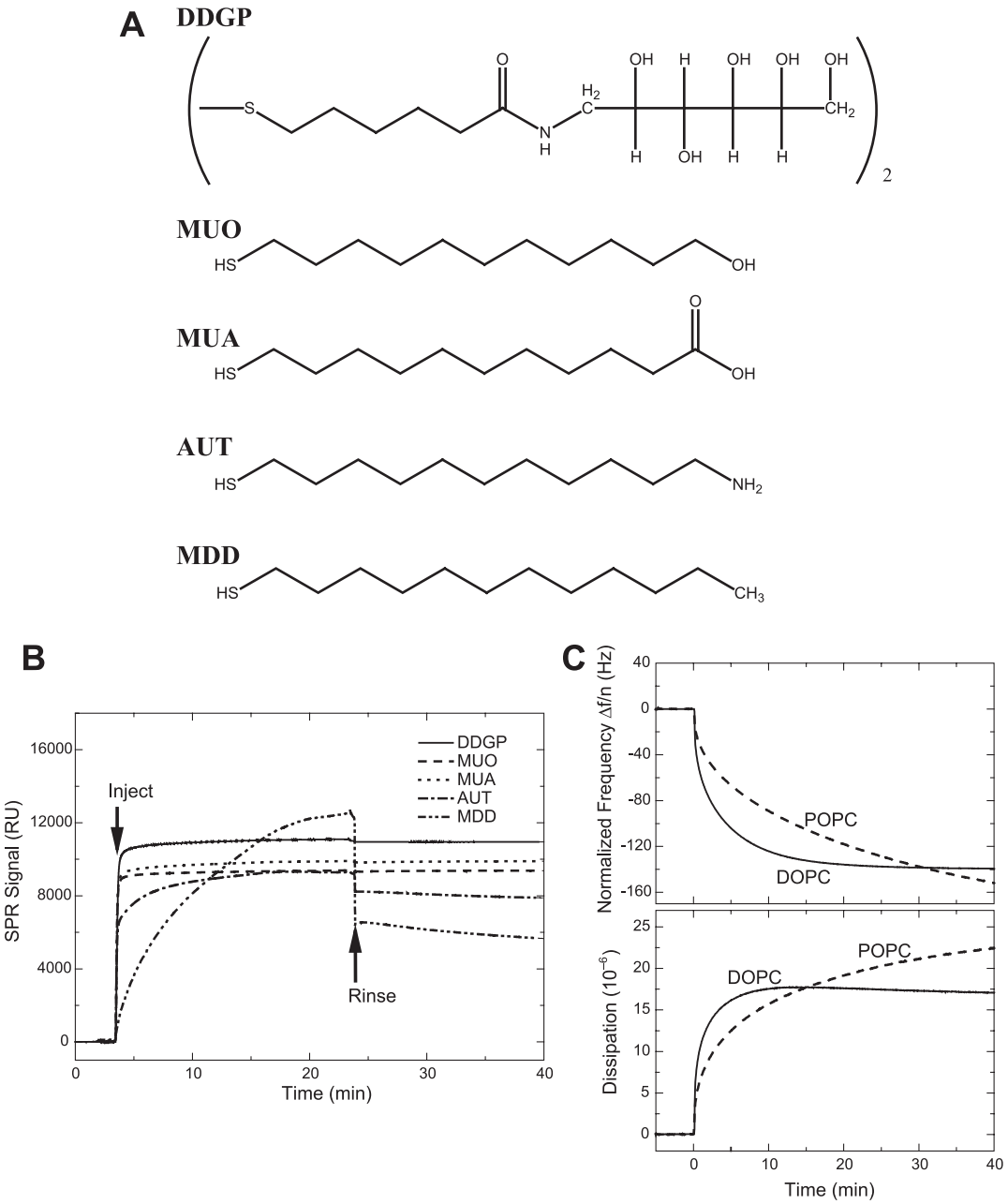


FIG. 3. (A) Chemical structures of thiol and disulfide derivatives to form SAMs on Biacore SIA Au sensor chips. DDGP, dithiobis(1-deoxy-D-glucitol-1-carbamoyl pentane); MUO, 11-mercaptoundecanol; MUA, 11-mercaptoundecanoic acid; AUT, 11-amino-1-undecanethiol; MDD, 12-mercaptododecane. (B) Time courses of SPR signal due to adsorption of DOPC vesicle on SAMs. At injection, 100 µl of 1 mg ml$^{-1}$ DOPC unilamellar vesicle was applied at a flow rate of 5 µl min$^{-1}$. Just after the injection ended, the sensor surface was rinsed with a running buffer composed of 0.15 M NaCl, 10 mM Tris–HCl (pH 7.4) and 2 mM $CaCl_2$ at a flow rate of 1.5 ml min$^{-1}$ for 10 s and, subsequently, a flow rate of 5 µl min$^{-1}$. Temperature, 25.0°C. (C) Temporal changes in shifts in normalized resonance frequency and dissipation due to adsorption of DOPC and POPC vesicles on DDGP SAM. An aqueous suspension of 0.1 mg ml$^{-1}$ DOPC or POPC suspended in the running buffer was applied to the flow chamber of the QCM-D instrument. Temperature: 25.0°C.

nance frequency and dissipation reached saturation within 20 min, and consequently, the resonance frequency decreased by 139 Hz and the dissipation increased by $17\times10^{-6}$ (Fig. 3C). The temporal changes in the resonance frequency and dissipation are very similar to those for the formation of the phospholipid vesicle layer on oxidized gold surface such that the intact phospholipid vesicle adsorbs on the surface as reported previously (12). Moreover, the saturation of both values suggests that a full coverage of DDGP SAM by the DOPC vesicle should occur within tens of minutes after the DOPC vesicle injection, and further adsorption of the DOPC vesicle would be prohibited by the full coverage. In addition, the standard deviation of the SPR signal during rinsing with the running buffer was 1.63 RU within the interval of 1000 s, which is 0.015% of the SPR signal value at saturation 11,000 RU suggesting that the DOPC vesicle layer is

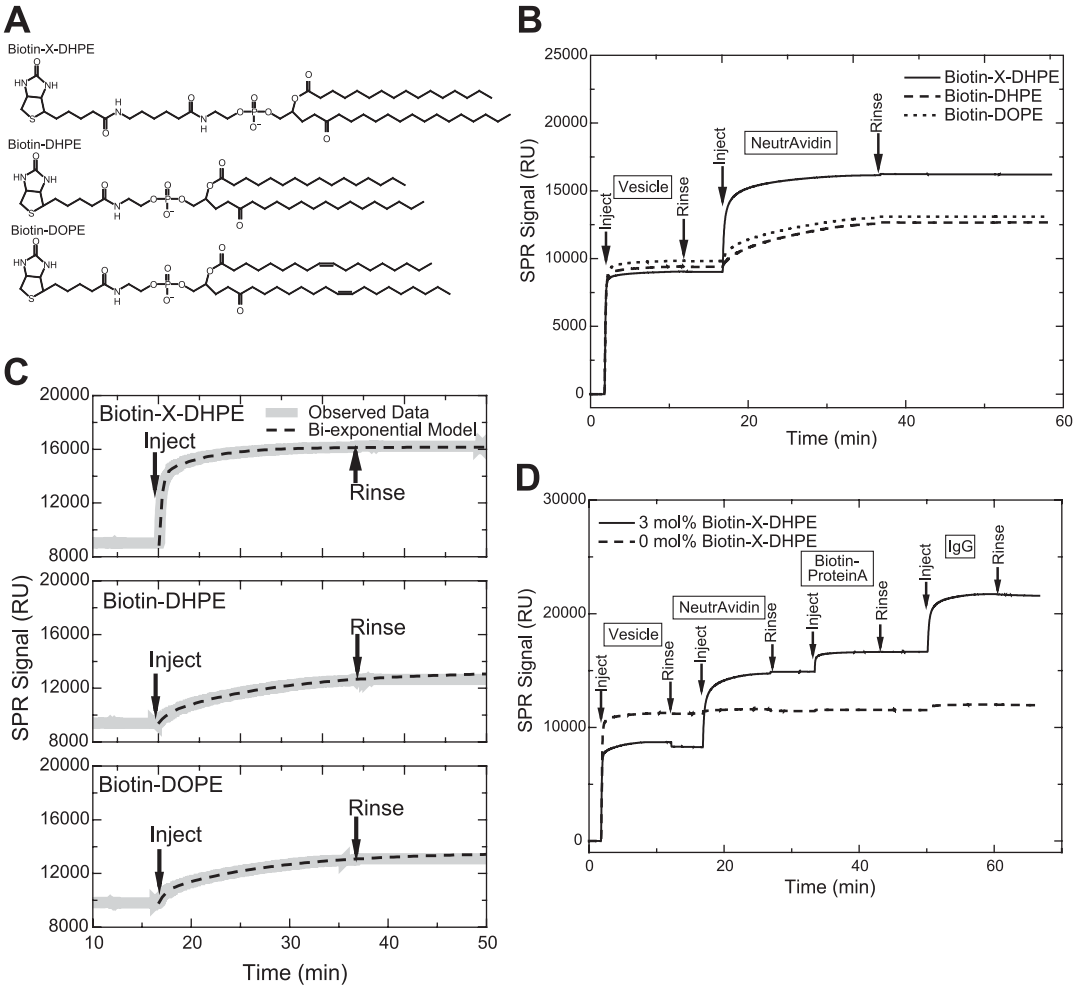


FIG. 4. Binding of NeutrAvidin to biotin-containing vesicle layers. (A) Chemical structures of biotinylated phospholipids mixed in DOPC to form vesicle layers on DDGP SAM. (B) Time courses of SPR signal change due to sequential injections of vesicle containing biotinylated phospholipid and NeutrAvidin. One of the three biotinylated phospholipids shown in panel A was mixed at a molar fraction of 3% in DOPC to obtain a biotin-containing vesicle suspension at a concentration of 1 mg ml$^{-1}$ phospholipid. After the injection of 50 μl of the vesicle suspension, 100 μl of 1 mg ml$^{-1}$ NeutrAvidin was injected. Temperature: 25.0°C. (C) Nonlinear least-square fitting of SPR signal changes with a bi-exponential function. The SPR signal curve was fitted with a function, $y_0 - A_1 \exp(-k_1(t-t_0)) - A_2 \exp(-k_2(t-t_0))$, where $y_0$ is an SPR signal when the binding of NeutrAvidin reaches a plateau, $t_0$ is the time when the injection of NeutrAvidin was started, and $A_1$ and $A_2$ are the increases in SPR signal due to the binding of NeutrAvidin to the biotin-containing vesicle layer at rate constants of $k_1$ and $k_2$, respectively. (D) SPR signal changes due to injection of vesicle suspension of 3 mol% biotin-X-DHPE mixed in DOPC (indicated as 3 mol% Biotin-X-DHPE) or DOPC without biotin-X-DHPE (indicated as 0 mol% Biotin-X-DHPE), followed by sequential injections of NeutrAvidin, biotinylated protein A, and IgG. The injections were made with 50 μl of 1 mg ml$^{-1}$ phospholipid vesicle, 1 mg ml$^{-1}$ NeutrAvidin, 0.1 mg ml$^{-1}$ biotinylated protein A, and 0.1 mg ml$^{-1}$ IgG. Temperature: 25.0°C.

very stable under the flow of the running buffer. Moreover, the adsorption of the vesicle of POPC, another widely used phospholipid in supported lipid membrane studies, was also examined by QCM-D for comparison. In contrast with DOPC, the shifts in the resonance frequency and dissipation for the injection of the POPC vesicle seem not to reach plateaus during the observation time of 40 min (Fig. 3C).

**Biotin-containing phospholipid vesicle layer for biosensing** The vesicle layer of a mixture of biotinylated phospholipid and DOPC was prepared on the DDGP SAM, and the binding of NeutrAvidin to the vesicle layer was investigated by SPR. A suspension of unilamellar vesicle was prepared from 3 mol% biotin-X-DHPE, biotin-DHPE or biotin-DOPE (Fig. 4A) mixed with DOPC. The resulting vesicle suspension was applied to DDGP SAM to form biotin-X-DHPE/DOPC, biotin-DHPE/DOPC or biotin-DOPE/DOPC vesicle layer, and the binding of NeutrAvidin with the biotin-containing phospholipid vesicle layer was monitored by SPR. Figure 4B shows that these biotinylated phospholipid/DOPC mixture vesicles adsorb on the DDGP SAM with SPR signal increases comparable to that of DOPC alone (Fig. 3B), suggesting that the vesicle layers of the mixtures are likely to be formed on the DDGP SAM in a manner similar to the DOPC vesicle layer. Additionally, it was observed that NeutrAvidin bound to these biotin-containing vesicle layers (Fig. 4B).

The change in the SPR signal responsible for the binding of NeutrAvidin to the biotin-containing vesicle layer was found to be dependent on the type of biotinylated phospholipid mixed with DOPC. To investigate the binding, the time

TABLE 1. Kinetic parameters of binding of NeutrAvidin to biotin-containing vesicle layers calculated by nonlinear least-square estimation with a bi-exponential function

| Biotinylated phospholipid mixed in DOPC | Rapid binding | | Slow binding | |
|---|---|---|---|---|
| | $k_1$ (min$^{-1}$) | $A_1$ (RU) | $k_2$ (min$^{-1}$) | $A_2$ (RU) |
| Biotin-X-DHPE | 3.7 | 4150 | 0.22 | 2040 |
| Biotin-DHPE | 1.1 | 553 | 0.085 | 3200 |
| Biotin-DOPE | 1.5 | 749 | 0.089 | 2900 |

course of the SPR signal was analyzed by a nonlinear least-square method with exponential functions. The changes in the SPR signal for the three biotin-containing phospholipid vesicle layers were fit well with a bi-exponential function (Fig. 4C), whereas the fit with a single exponential was poor. The bi-exponential nature of NeutrAvidin binding indicates that the binding of NeutrAvidin to the biotin-containing phospholipid vesicle layers occurs at two binding rates. The binding rate constants and the corresponding increases in the SPR signal derived by the nonlinear least-square estimation are summarized in Table 1. The parameters of $k_1$ and $k_2$ are pseudo-first-order rate constants of the binding of NeutrAvidin to the biotinylated phospholipid measured at 1 mg ml$^{-1}$ NeutrAvidin. The increases in the SPR signal, $A_1$ and $A_2$, must relate to the amount of NeutrAvidin that binds to the biotin-containing vesicle layer at the rate constants of $k_1$ and $k_2$, respectively. For the biotin-X-DHPE/DOPC vesicle layer, the rapid binding phase is dominant in that $A_1$ is 2-fold higher than $A_2$, whereas for the biotin-DHPE/DOPC and biotin-DOPE/DOPC vesicle layers, the slow binding phase is dominant, because their $A_1$ values are much lower than their $A_2$ values. Moreover, the SPR signal increases in the total NeutrAvidin binding, $(A_1+A_2)$, for the biotin-DHPE/DOPC and biotin-DOPE/DOPC vesicle layers are substantially lower than that of biotin-X-DHPE/DOPC layers. Thus, the present investigation demonstrates that the use of biotin-X-DHPE achieves a more rapid immobilization of NeutrAvidin on the phospholipid vesicle layer at a higher surface density, and biotin-X-DHPE must be more suitable for high-throughput and highly sensitive biosensing applications than biotin-DHPE and biotin-DOPE.

Furthermore, on the NeutrAvidin-bound biotin-X-DHPE/DOPC vesicle layer prepared as mentioned above, a biotinylated receptor protein was immobilized by the biotin-avidin chemistry, and the reaction between the receptor and an analyte protein was examined by SPR. As a model system, we used biotinylated protein A and immunoglobulin G (IgG) for the receptor and analyte proteins, respectively (Fig. 1). Figure 4D shows the SPR signal changes of 6600, 1800 and 4900 RU for sequential injections of NeutrAvidin, biotinylated protein A and IgG, respectively. The amounts of proteins bound to the sensor chip surface are computed as 660, 180 and 490 ng/cm$^2$, respectively, if we can use a correlation coefficient of 0.1 ng/cm$^2$/RU between the SPR signal change and the amount of bound protein (33). In contrast, for the DOPC membrane devoid of biotin-X-DHPE, the SPR signal increases for the injections of NeutrAvidin, biotinylated protein A and IgG were significantly lower: 230, 93 and 430 RU, respectively (Fig. 4D). The SPR signal changes roughly correspond to 23, 9.3 and 43 ng/cm$^2$, respectively. These results demonstrate that the protein molecules can be immobilized on the biotin-X-DHPE/DOPC vesicle layer almost through specific interaction, and the vesicle layer is resistant to nonspecific protein adsorption.

**Optimization of biotin-X-DHPE content** To optimize the biotin-X-DHPE/DOPC vesicle layer for the immobilization of the biotinylated receptor protein on the layer, we examined the molar fraction of biotin-X-DHPE contained in the vesicle layer on the DDGP SAM. Unilamellar vesicles of 0–100 mol% biotin-X-DHPE mixed with DOPC were prepared and applied onto DDGP SAM. The binding reactions of NeutrAvidin, biotinylated protein A and then IgG on the biotin-containing vesicle layer were measured using SPR similarly to Fig. 4D. The increases in the SPR signal due to binding are summarized in Fig. 5. As the biotin-X-DHPE fraction increases up to 3 mol%, the SPR signal changes for the binding of the three proteins rapidly increases. However, the SPR signal increases are less affected in the range of 3–30 mol% biotin-X-DHPE. Thus, these results indicate that biotin-X-DHPE of a fraction of approximately 3 mol% is necessary for maximizing the surface densities of the immobilized proteins and thereby obtaining a high sensitivity for the detection of the analyte protein. Additionally, the SPR signal change due to the adsorption of biotin-X-DHPE/DOPC vesicle decreases as the biotin-X-DHPE fraction increases, and the vesicle of 100 mol% biotin-X-DHPE fails to adsorb onto the DDGP SAM (Fig. 5). This decrease in the SPR signal might suggest an increase in the number of defects in the phospholipid vesicle layer with the increased fraction of biotin-X-DHPE. Thus, the biotin-X-DHPE fraction of approximately 3 mol% may be the optimum condition for the biotin-X-DHPE/DOPC vesicle layer on the DDGP SAM for SPR biosensing, although the sensitivity for detecting the proteins was observed to be insignificantly affected in the

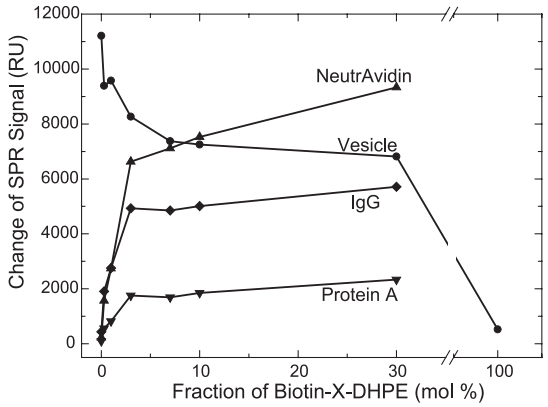


FIG. 5. Profile of SPR signal increases due to the injections of vesicles, NeutrAvidin, biotinylated protein A and IgG as functions of molar percentage of biotin-X-DHPE mixed in DOPC.

range of 3–30 mol% biotin-X-DHPE. Similarly to the present study, it has been reported that the binding of streptavidin to a mixed SAM of MUO and a biotinylated thiolate is dependent on the molar fraction of the biotinylated thiolate, and was found to be optimum at 15 mol% biotinylated thiolate (34).

## DISCUSSION

In the study, we demonstrated the method of immobilizing biotinylated protein A on the SPR sensor chip using the biotin-containing phospholipid vesicle layer through the biotin-avidin-biotin linkage. Additionally, IgG was allowed to bind to the protein A on the vesicle layer, *i.e.*, IgG was immobilized through the biotinylated protein A. Moreover, it should be noted that the vesicle layer exhibited resistance to nonspecific protein adsorption. Therefore, the present method should be useful for producing the surface layer of an antibody SPR biosensor containing IgG on the sensor surface. Otherwise, immunoglobulin labeled with a biotinylation reagent can be directly immobilized on the NeutrAvidin-bound biotin-containing vesicle layer.

As a further application, the phospholipid vesicle layers on the gold surface can be combined with fluorescence measurement. The fluorescence of fluorescent molecules in the vicinity of the gold surface is known to be substantially quenched owing to the energy transfer from the dyes to gold (21), and this would often be problematic when observing the SPR-enhanced fluorescence of the dyes. However, if a phospholipid vesicle layer is formed on the surface of an SPR biosensor, the fluorescent analyte and/or receptor molecules will be separated from the gold surface, thereby decreasing the quenching effect. Thus, by using the phospholipid vesicle layer, simultaneous measurements of fluorescence and SPR (21, 35) would be achieved with a high sensitivity. In fact, SPR can be used to measure protein-protein interactions with a high sensitivity, but does not have sufficient sensitivity for measuring the binding of small-molecule ligands, *e.g.*, ATP, GTP, cyclic AMP, acetylcholine and peptide hormones, to receptor proteins. However, if the small-molecule ligands are fluorescently labeled, the SPR-enhanced fluorescence measurement can enable the detection of the binding of the small-molecule ligands to proteins at a high sensitivity. Thus, with the phospholipid vesicle layer formed on the surface of the SPR sensor chip, the simultaneous measurements of SPR and SPR-enhanced fluorescence would be useful for analyzing protein-protein interactions that are dependent on small-molecule ligands.

The kinetics of the adsorption of phospholipid vesicle on the SAMs was observed to be dependent on the chemical species constituting the SAM. By the injection of the DOPC vesicle, the SPR signal reached a plateau rapidly for the SAMs of DDGP, MUO and MUA (Fig. 3B). Considering that the DOPC vesicle layer was formed on the DDGP SAM and the SPR signal changes due to the injection of the DOPC vesicle for the SAMs of DDGP, MUO and MUA were similar, the DOPC vesicle layer is most likely to be formed also on the surfaces of the MUO and MUA SAMs. However, the SPR signal for the DDGP SAM was the highest among the three SAMs, and this suggested that the highest coverage of the sensor chip surface with the DOPC vesicle layer may be achieved on the DDGP SAM. Thus, the DDGP SAM was chosen for this study.

QCM-D measurement showed that both resonance frequency and dissipation exhibited plateaus after the injection of the DOPC vesicle (Fig. 3C). The temporal changes in the signals indicated that the DOPC vesicle did not accumulate on the DOPC vesicle layer, after the vesicle layer formed on the DDGP SAM. In contrast, the resonance frequency and dissipation for the injection of the POPC vesicle did not reach saturation within the interval (40 min) of the QCM-D experiment (Fig. 3C). These results suggest that the DOPC vesicle interacts more strongly with the surface of the DDGP SAM and less favorably with the DOPC vesicles themselves than the POPC vesicle does. Because of the properties of the DOPC vesicle, DOPC, rather than POPC, was chosen for preparing the phospholipid vesicle layer on the DDGP SAM in this study.

A plateau of the amount of NeutrAvidin bound to biotin-X-DHPE/DOPC vesicle layer was observed for ≥3 mol% biotin-X-DHPE (Fig. 5). This may arise from the saturation of the bound NeutrAvidin molecule on the vesicle layer surface. If we use the correlation coefficient of 0.1 ng/cm$^2$ protein adsorption per 1 RU (33), although its measurement condition was not the same as that of the present study, the number of NeutrAvidin molecules per square area of the side length of 10 nm on the sensor chip surface is computed from the SPR signal of 6600 RU at 3 mol% biotin-X-DHPE (Fig. 5) as

$$\frac{0.1\times10^{-9}\times6600}{60000}\times(10\times10^{-7})^2\times6.02\times10^{23} = 6.6\ (\text{molecules}/100\ \text{nm}^2) \quad (2)$$

where 60,000 is the molecular weight of NeutrAvidin. To examine the surface area of the phospholipid vesicle accessible to NeutrAvidin, by an approximation, we consider a close-packed layer of spherical phospholipid vesicle with a radius $r$. If we assume that the vesicle is not deformed notwithstanding its adsorption on the SAM surface and that NeutrAvidin is accessible to the upper half of the vesicle, the total surface area of the phospholipid vesicles accessible from NeutrAvidin in the square region of the sensor chip surface with a side length $L$ is expressed as

$$\frac{L}{2r}\times\frac{4\pi r^2}{2}=\frac{\pi L^2}{2}=1.57\,L^2 \quad (3)$$

This indicates that, in this approximation, the surface area of vesicles accessible from NeutrAvidin in a square region of the sensor chip surface is not dependent on the vesicle radius and only 1.57 times the area of the square region. Thus, the surface density of the NeutrAvidin molecule on the phospholipid vesicle surface will be 6.6/1.57 = 4.2 molecules/100 nm$^2$. If we consider the diameter of NeutrAvidin as approximately 5 nm, the NeutrAvidin molecules on the biotin-containing vesicle layer would be near by close-packed. Furthermore, an SPR signal of 1 RU was reported to correspond to 0.092 ng/cm$^2$ of adsorbed egg phosphatidylcholine (36), and, if this correlation is used for the biotin-X-DHPE/DOPC vesicle layer by a crude estimation, the surface den-

sity of the biotin-X-DHPE molecule on the sensor chip surface for the biotin-X-DHPE/DOPC vesicle layer of 3 mol% biotin-X-DHPE is calculated as

$$0.25 \times 0.03 \times \frac{0.092 \times 10^{-9} \times 8300}{0.03 \times 1028.43 + 0.97 \times 786.11} \times (10 \times 10^{-7})^2 \times 6.02 \times 10^{23} = 4.3 \text{ (molecules/100 nm}^2\text{)} \quad (4)$$

where the values of 1023.43 and 786.11 are the molecular weights of biotin-X-DHPE and DOPC, respectively, and the value of 8300 is the SPR signal change corresponding to the vesicle adsorption (Fig. 5). The factor of 0.25 arises from the assumption that only the outer surface of the upper half of the spherical phospholipid vesicle is accessible to NeutrAvidin. According to the approximation stated above, the density of the biotin-X-DHPE molecule accessible to NeutrAvidin with regard to the phospholipid vesicle surface will be 4.3/1.57 = 2.8 molecules/100 nm$^2$. This estimated value is in the same order as that of NeutrAvidin notwithstanding such crude estimation. Considering these calculations, the plateau of the amount of bound NeutrAvidin for ≥3 mol% biotin-X-DHPE (Fig. 5) is likely to be due to the close packing of NeutrAvidin on the surface of biotin-X-DHPE/DOPC vesicle layer.

The kinetic parameters of the NeutrAvidin binding for the biotin-DHPE/DOPC and biotin-DOPE/DOPC vesicle layers were very similar to each other, but different from that for the biotin-X-DHPE/DOPC vesicle layer (Table 1). Biotin-X-DHPE and biotin-DHPE have the same hydrocarbon tail chains, and biotin-DHPE and biotin-DOPE have the same polar head group (Fig. 4A). However, the 6-amino-hexanoate moiety is inserted between the biotin and ethanolamine in the polar portion of biotin-X-DHPE, unlike in the case of biotin-DHPE and biotin-DOPE. Considering the structures of the biotinylated phospholipids and the kinetic properties, it is suggested that the linker length between the phosphor atom and biotinyl group would have a primary effect on the binding of NeutrAvidin to the biotinylated phospholipid. Furthermore, the linker length may have an effect on the motional freedom of the NeutrAvidin molecules bound to the biotin-containing vesicle layer, and the motional freedom of NeutrAvidin may affect the packing of NeutrAvidin molecules, resulting in the lower surface density of the NeutrAvidin molecule on the biotin-DHPE/DOPC and biotin-DOPE/DOPC vesicle layers, and thus, the lower value of the SPR signal at saturation, *i.e.*, ($A_1$+$A_2$). In fact, the density of the bound NeutrAvidin molecule on the vesicle layer surface at saturation was estimated to be near by close-packed, as discussed above. Moreover, the lower reaction rates of NeutrAvidin binding, $k_1$ and $k_2$, for biotin-DHPE and biotin-DOPE than for biotin-X-DHPE may be due to an electric or steric repulsion force exerting between the NeutrAvidin molecule and vesicle surface because of their shorter linker between the biotinyl group and phosphor atom.

The binding of NeutrAvidin to the biotin-containing phospholipid vesicle layers was observed to occur with the bi-exponential kinetics (Fig. 4C). To the best of our knowledge, the bi-exponential kinetics of avidin-class proteins to the biotin-containing substrate surfaces has not been reported, although the dissociation of streptavidin from a mixed SAM of MUO and a biotinylated thiolate has been reported to follow a bi-exponential kinetics, suggesting that this arose from the multivalence of streptavidin for biotin binding (34, 37). As computed from Table 1, the ratios of $A_1/A_2$ for biotin-X-DHPE/DOPC, biotin-DHPE/DOPC and biotin-DOPE/DOPC vesicle layers are 2.0, 0.17 and 0.25, respectively, and thus, the amounts of NeutrAvidin that react through the slow and fast binding phases strongly depend on the linker length between the biotinyl group and phosphor atom. Although the mechanism of the bi-exponential kinetics is still unknown at present, the results suggest that the bi-exponential kinetics of NeutrAvidin binding observed in this study is related closely to the linker length, rather than the multivalence of biotin binding for NeutrAvidin or the geometry of phspholipid vesicles adsorbed on the DDGP SAM. As the binding of NeutrAvidin to the biotin-containing vesicle layer proceeds, the surface of the vesicle layer will be covered with NeutrAvidin molecules. The NeutrAvidin binding would thus be sterically hindered, as the binding reaction proceeds. Because the motional freedom of NeutrAvidin molecules bound to the biotin-DHPE/DOPC and biotin-DOPE/DOPC vesicle layers would be lower than that to the biotin-X-DHPE/DOPC vesicle layer; the steric hindrance of NeutrAvidin binding to the biotin-DHPE/DOPC and biotin-DOPE/DOPC vesicle layers would be expected to be larger. In fact, the amount of bound NeutrAvidin through the slow binding phase ($A_2$ in Table 1) is much higher than that through the fast phase ($A_1$ in Table 1) for biotin-DHPE/DOPC and biotin-DOPE vesicle layers, as expected from the consideration. Thus, the steric crowding effect may account for the bi-exponential kinetics, although other possibilities may not be ruled out.

SAMs of saccharide-terminated molecular species on gold have been described by several research groups. The terminal groups of the alkyl thiols were glucose, mannitol and galactose, and these SAMs have been shown to be highly protein-resistant and inert to cells (38–41). In this study, we synthesized a novel saccharide-terminated alkyl disulfide, DDGP, and moreover, the DOPC vesicle layer was demonstrated to be formed on the DDGP SAM. To the best of our knowledge, this is the first report that demonstrates that phospholipid vesicle layers can be formed on the SAM of a saccharide-terminated derivative, and a biomolecular interaction that takes place on the vesicle layer can be detected by SPR.

## ACKNOWLEDGMENTS

We thank Dr. Frank Brozovich (Mayo Clinic) and Dr. Yuko Takeuchi (PRESTO: Innovative Nanotechnology Integration, JST) for critical reading of the manuscript. We are also grateful to Dr. Ken-ichi Shinohara (Japan Advanced Institute of Science and Technology) for his advice in the purification of DDGP, and Ms Rie Masuda (Graduate School of Frontier Biosciences, Osaka University) for her assistance in the analysis of $^1$H-NMR spectra. This work was partly supported by a grant-in-aid from the Ministry of Education, Culture, Sports, Science and Technology (project no. 16201030).

## REFERENCES


1. **Marquette, C. A. and Blum, L. J.:** State of the art and recent advances in immunoanalytical systems. Biosens. Bioelectron., **21**, 1424–1433 (2006).
2. **Löfås, S., Malmqvist, M., Rönnberg, I., Stenberg, E., Liedberg, B., and Lundström, I.:** Bioanalysis with surface-plasmon resonance. Sens. Actuators B Chem., **5**, 79–84 (1991).
3. **Brockman, J. M., Nelson, B. P., and Corn, R. M.:** Surface plasmon resonance imaging measurements of ultrathin organic films. Annu. Rev. Phys. Chem., **51**, 41–63 (2000).
4. **Tomizaki, K., Usui, K., and Mihara, H.:** Protein-detecting microarrays: current accomplishments and requirements. ChemBioChem, **6**, 782–799 (2005).
5. **Sackmann, E.:** Supported membranes: scientific and practical applications. Science, **271**, 43–48 (1996).
6. **Boxer, S. G.:** Molecular transport and organization in supported lipid membranes. Curr. Opin. Chem. Biol., **4**, 704–709 (2000).
7. **Groves, J. T. and Boxer, S. G.:** Micropattern formation in supported lipid membranes. Acc. Chem. Res., **35**, 149–157 (2002).
8. **Tanaka, M. and Sackmann, E.:** Polymer-supported membranes as models of the cell surface. Nature, **437**, 656–663 (2005).
9. **Brian, A. A. and McConnell, H. M.:** Allogeneic stimulation of cytotoxic T cells by supported planar membranes. Proc. Natl. Acad. Sci. USA, **81**, 6159–6163 (1984).
10. **Nollert, P., Kiefer, H., and Jähnig, F.:** Lipid vesicle adsorption versus formation of planar bilayers on solid surfaces. Biophys. J., **69**, 1447–1455 (1995).
11. **Richter, R. P., Bérat, R., and Brisson, A. R.:** Formation of solid-supported lipid bilayers: an integrated view. Langmuir, **22**, 3497–3505 (2006).
12. **Keller, C. A. and Kasemo, B.:** Surface specific kinetics of lipid vesicle adsorption measured with a quartz crystal microbalance. Biophys. J., **75**, 1397–1402 (1998).
13. **Richter, R. P., Him, J. L. K., and Brisson, A.:** Supported lipid membranes. Mater. Today, **6**, 32–37 (2003).
14. **Burgess, I., Li, M., Horswell, S. L., Szymanski, G., Lipkowski, J., Satija, S., and Majewski, J.:** Influence of the electric field on a bio-mimetic film supported on a gold electrode. Colloids Surf. B Biointerfaces, **40**, 117–122 (2005).
15. **Plant, A. L.:** Self-assembled phospholipid/alkanethiol biomimetic bilayers on gold. Langmuir, **9**, 2764–2767 (1993).
16. **Gizeli, E., Liley, M., Lowe, C. R., and Vogel, H.:** Antibody binding to a functionalized supported lipid layer: a direct acoustic immunosensor. Anal. Chem., **69**, 4808–4813 (1997).
17. **Schouten, S., Stroeve, P., and Longo, M. L.:** DNA adsorption and cationic bilayer deposition on self-assembled monolayers. Langmuir, **15**, 8133–8139 (1999).
18. **Melzak, K., Ralph, E., and Gizeli, E.:** Effect of the surface hydrophilicity on the formation of a membrane-type interface: study using an acoustic wave device. Langmuir, **17**, 1594–1598 (2001).
19. **Ekeroth, J., Konradsson, P., and Höök, F.:** Bivalent-ion-mediated vesicle adsorption and controlled supported phospholipid bilayer formation on molecular phosphate and sulfate layers on gold. Langmuir, **18**, 7923–7929 (2002).
20. **Wang, Z., Wilkop, T., and Cheng, Q.:** Characterization of micropatterned lipid membranes on a golf surface by surface plasmon resonance imaging and electrochemical signaling of a pore-forming protein. Langmuir, **21**, 10292–10296 (2005).
21. **Tawa, K. and Morigaki, K.:** Substrate-supported phospholipid membranes studied by surface plasmon resonance and surface plasmon fluorescence spectroscopy. Biophys., J., **89**, 2750–2758 (2005).
22. **Phillips, K. S., Han, J. H., Martinez, M., Wang, Z., Carter, D., and Cheng, Q.:** Nanoscale glassification of gold substrates for surface plasmon resonance analysis of protein toxins with supported lipid membranes. Anal. Chem., **78**, 596–603 (2006).
23. **Schmidt, E. K., Liebermann, T., Kreiter, M., Jonczyk, A., Naumann, R., Offenhäusser, A., Neumann, E., Kukol, A., Maelicke, A., and Knoll, W.:** Incorporation of the acetylcholine receptor dimer from Torpedo californica in a peptide supported lipid membrane investigated by surface plasmon and fluorescence spectroscopy. Biosens. Bioelectron., **13**, 585–591 (1998).
24. **Zhang, L., Booth, C. A., and Stroeve, P.:** Phosphatidylserine/cholesterol bilayers supported on a polycation/alkylthiol layer pair. J. Colloid Interface Sci., **228**, 82–89 (2000).
25. **Zhang, L., Longo, M. L., and Stroeve, P.:** Mobile phospholipid bilayers supported on a polyion/alkylthiol layer pair. Langmuir, **16**, 5093–5099 (2000).
26. **Rongen, H. A. H., Bult, A., and Van Bennekom, W. P.:** Liposomes and immunoassays. J. Immunol. Methods, **204**, 105–133 (1997).
27. **Sofou, S. and Thomas, J. L.:** Stable adhesion of phospholipid vesicles to modified gold surfaces. Biosens. Bioelectron., **18**, 445–455 (2003).
28. **Yoshina-Ishii, C. and Boxer, S. G.:** Arrays of mobile tethered vesicles on supported lipid bilayers. J. Am. Chem. Soc., **125**, 3696–3697 (2003).
29. **Städler, B., Falconnet, D., Pfeiffer, I., Höök, F., and Vörös, J.:** Micropatterning of DNA-tagged vesicles. Langmuir, **20**, 11348–11354 (2004).
30. **Williams, T. L., Vareiro, M. M. L. M., and Jenkins, A. T. A.:** Fluorophore-encapsulated solid-supported bilayer vesicles: a method for studying membrane permeation processes. Langmuir, **22**, 6473–6476 (2006).
31. **MacDonald, R. C., MacDonald, R. I., Menco, B. P. M., Takeshita, K., Subbarao, N. K., and Hu, L.:** Small-volume extrusion apparatus for preparation of large unilamellar vesicles. Biochim. Biophys. Acta, **1061**, 297–303 (1991).
32. **Hermanson, G. T.:** Bioconjugate techniques. Academic Press, San Diego (1995).
33. **Stenberg, E., Persson, B., Roos, H., and Urbaniczky, C.:** Quantitative determination of surface concentration of protein with surface plasmon resonance by using radiolabeled proteins. J. Colloid Interface Sci., **143**, 513–526 (1991).
34. **Pérez-Luna, V. H., O'Brien, M. J., Opperman, K. A., Hampton, P. D., López, G. P., Klumb, L. A., and Stayton, P. S.:** Molecular recognition between genetically engineered streptavidin and surface-bound biotin. J. Am. Chem. Soc., **121**, 6469–6478 (1999).
35. **Liebermann, T., Knoll, W., Sluka, P., and Hermann, R.:** Complement hybridization from solution to surface-attached probe-oligonucleotides observed by surface-plasmon-field-enhanced fluorescence spectroscopy. Colloids Surface A Physicochem. Eng. Asp., **169**, 337–350 (2000).
36. **Cooper, M. A., Try, A. C., Carroll, J., Ellar, D. J., and Williams, D. H.:** Surface plasmon resonance analysis at a supported lipid monolayer. Biochim. Biophys. Acta, **1373**, 101–111 (1998).
37. **Jung, L. S., Nelson, K. E., Campbell, C. T., Stayton, P. S., Yee, S. S., Pérez-Luna, V., and López, G. P.:** Surface plasmon resonance measurement of binding and dissociation of wild-type and mutant streptavidin on mixed biotin-containing alkylthiolate monolayers. Sens. Actuators B Chem., **54**, 137–144 (1999).
38. **Prime, K. L. and Whitesides, G. M.:** Self-assembled organic monolayers: model systems for studying adsorption of proteins at surfaces. Science, **252**, 1164–1167 (1991).
39. **Kitov, P. I., Railton, C., and Bundle, D. R.:** The synthesis of 16-mercaptohexadecanyl glycosides for biosensor applications. Carbohydr. Res., **307**, 361–369 (1998).
40. **Luk, Y., Kato, M., and Mrksich, M.:** Self-assembled monolayers of alkanthiolates presenting mannitol groups are inert to protein adsorption and cell attachment. Langmuir, **16**, 9604–9608 (2000).
41. **Hederos, M., Konradsson, P., and Liedberg, B.:** Synthesis and self-assembly of galactose-terminated alkanethiols and their ability to resist proteins. Langmuir, **21**, 2971–2980 (2005).